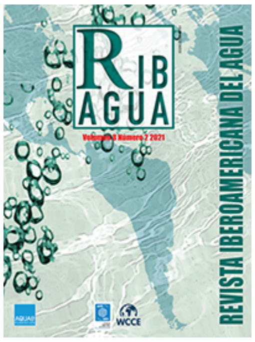

Ribagua

Revista Iberoamericana del Agua

ISSN: (Print) (Online) Journal homepage: iahr.tandfonline.com/journals/trib20

Yield strength determination from slump test

Rodrigo Mosquera & Francisco Pedocchi

To cite this article: Rodrigo Mosquera & Francisco Pedocchi (2021) Yield strength determination from slump test, Ribagua, 8:2, 35-40, DOI: 10.1080/23863781.2022.2147461

To link to this article: https://doi.org/10.1080/23863781.2022.2147461

Published online: 23 Nov 2022.

RIBAGUA
2021, VOL. 8, NO. 2, 35–40
https://doi.org/10.1080/23863781.2022.2147461

Yield strength determination from slump test

Rodrigo Mosquera and Francisco Pedocchi

Instituto de Mecánica de los Fluidos e Ingeniería Ambiental, Facultad de Ingeniería, Universidad de la República, Uruguay

ABSTRACT

The routinely determination of the yield strength of muddy beds is particularly important for the assessment of navigation in ports located in estuaries where cohesive sediments are abundant. The use of the nautical bottom concept may allow for a significant increase of the navigation depth. Sediments mixtures rich in clay and silt could behave as either a solid or a fluid depending on the forces acting on them. A concentrated mud sample will retain its shape if subject to shear stresses bellow the yield strength. However, if the same sample is subject to shear stresses above the yield strength, it will flow. One simple way of determining the yield strength is by performing a slump test. In this work, instead of just measuring the deposit final height or radius, as it has been done in the past, we fit an analytical expression to the deposit final geometry to estimate the yield strength. Simultaneous yield strength measurements using a conventional vane rheometer showed to be in very good agreement with the proposed technique independently of the mud sample origin, which is a clear improvement over the existing slump test methods, which just use the final height of the deposit.

RESUMEN

La determinación rutinaria de la tensión de cedencia de los barros presentes en el fondo marino es particularmente importante para la evaluación de la navegación en puertos ubicados en estuarios, donde los sedimentos cohesivos son abundantes. El uso del concepto del fondo náutico puede permitir un incremento significativo en las profundidades de navegación. Mezclas de sedimentos con mucha presencia de arcillas y limos pueden comportarse tanto como un sólido o como un fluido, dependiendo de los esfuerzos actuando sobre las mismas. Una muestra de barro concentrado mantendrá su forma si se encuentra sometido a tensiones rasantes menores a la tensión de cedencia. Sin embargo, si la misma muestra se encuentra sometida a tensiones rasantes por encima de la tensión de cedencia, la muestra fluirá. Una forma sencilla de determinar la tensión de cedencia es mediante el ensayo de asentamiento. En este trabajo, en lugar de solo medir la altura o radio final del depósito, como se propone en los ensayos de asentamiento tradicionales, se ajusta una expresión analítica a la geometría final para estimar la tensión de cedencia. Paralelamente se realizaron mediciones de la tensión de cedencia utilizando un reómetro de veleta, mostrando un muy buen ajuste con la técnica aquí propuesta independientemente del origen de la muestra de barro. Esto indica una mejora respecto a los ensayos de asentamiento tradicionales que solo utilizan la altura final del depósito.

ARTICLE HISTORY
Received 27 July 2022
Accepted 21 October 2022

KEYWORDS
Mud; yield strength; rheology; slump test

1. Introduction

There is a variety of materials that may manifest a solid or a fluid behavior depending on the forces they are exposed to. Sediments mixtures containing significant proportions of clay and silt, often called mud, present this behavior. A mud sample could retain its shape if subjected to shear stresses below a certain threshold, called yield strengthτ_Y. However, if the same sample is subjected to shear stresses above the yield strength, it will flow. During a slump test a mud sample previously placed into a bottomless container is quickly released. If the shear stresses introduced by the sample own weight exceed the material yield strength the sample will flow until the weight action is balanced by the shear forces acting inside the material and stresses acting on its boundaries. This process will leave a slump deposit with a particular shape, as shown on Figure 1, which results from the internal stress distribution inside the material at the instant just before the material stopped flowing.

Some of the rheological properties of a material are routinely estimated measuring the final deposit height H after the slump. For example, slump tests are used for fresh concrete quality control [1]. In this case, classification of the material is carried on by comparing the slump occurred when using a standardized truncated cone (10 cm upper diameter, 20 cm bottom diameter and 30 cm height) without top nor bottom. When

CONTACT Rodrigo Mosquera rmosquer@fing.edu.uy Instituto de Mecánica de los Fluidos e Ingeniería Ambiental, Facultad de Ingeniería, Universidad de la República, Uruguay

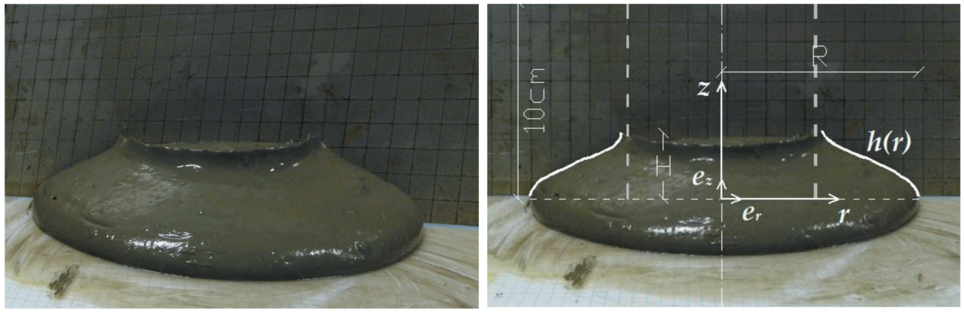

Figure 1. Photo of the slump test used to measure the final profile, original (left) and after rectification (right).

working with low resistance concretes, the mini-cone (7.6 *cm* of upper diameter, 10 *cm* bottom diameter and 10 *cm* height) test is used [2]. Similar tests are applied for quality control and sample comparison in the mining, food, and pharmaceutical industry [3,4]. However, for different materials the same final deposit height would not necessary be associated to one unique yield strength value. Furthermore, results obtained either with different container geometries or different surface roughness are not easily comparable, making it difficult to integrate results from different databases [5].

In the laboratory the yield strength of a material can be accurately measured using dedicated rheological equipment such as cone or vane rheometers. However, due to the small sample size they can handle, these rheometers present important limitations for the study of highly heterogeneous materials, which may contain large particles (mixes of mud with sand, gravel, or shells, for example). Moreover, rheometers are delicate and somehow expensive pieces of equipment, and it is not practical to carry them to the field during surveying works at sea. The technique described in this article solves several of the limitations described above and may be a useful tool for the determination of the nautical bottom in muddy ports and navigation channels.

2. Theory

Several researchers [4–11] have studied the motion of materials during the slumping process and have presented the basic equations for the relation between the final geometry of the deposit and the yield strength of the released material. The response of a particular material is determined by its constitutive equation, which relates internal stress at a point of the material, with local deformation and its time derivatives [12]. One of the simplest ways of representing a rheological material is using the *Bingham model*. A *Bingham material* has a visco-plastic behavior, having a solid body response for low shear stresses, and a viscous fluid response for shear stresses overpassing the yield strengthτ_Y. When the shear stress is equal toτ_Y, the material is said to be yielded or in yield state. The constitutive equation for a Bingham material is then expressed as [10]

$$\mathbf{D} = 0, \qquad \text{if } \tau < \tau_Y, \tag{1}$$

$$\tau = \left(\frac{\tau_Y}{D} + 2\mu\right)\mathbf{D}, \quad \text{if } \tau \geq \tau_Y, \tag{2}$$

where $\mathbf{D}$ is the strain rate tensor, D is$\sqrt{-I_{2D}}$, where $I_{2D} = \frac{1}{2}\left(\mathrm{tr}(\mathbf{D})^2 - \mathrm{tr}(\mathbf{D}^2)\right)$ the second invariant of $\mathbf{D}$, $\mathrm{tr}(\cdot)$the trace operator, $\tau$is the deviatoric stress tensor, $\tau$is$\sqrt{-I_{2\tau}}$, where $I_{2\tau}$ is second invariant ofτ, and μ the dynamic viscosity.

Assuming that the material is incompressible; that the flow solution has revolution symmetry; that the accelerations just before the end of material motion were very small, and therefore, the quasi-equilibrium approximation can be applied; and that the material is yielded at every point; then the governing equations can be written, using cylindrical coordinates, as

$$\mathrm{tr}(\mathbf{D}) = 0, \tag{3}$$

$$-\frac{\partial p}{\partial r} + \frac{\partial \tau_{rr}}{\partial r} + \frac{\partial \tau_{rz}}{\partial z} + \frac{\tau_{rr}}{r} = 0, \tag{4}$$

$$-\rho g - \frac{\partial p}{\partial z} + \frac{\partial \tau_{rz}}{\partial r} + \frac{\partial \tau_{zz}}{\partial z} + \frac{\tau_{rz}}{r} = 0, \tag{5}$$

$$\tau = \tau_Y, \tag{6}$$

where r is the horizontal radial distance from the center of the container, $z$is the upward vertical coordinate from the horizontal plane, $p$is the manometetric pressure, $\rho$is the material density, $g$is the acceleration of gravity, τ_{rr}, τ_{rz}, and τ_{zz} are the components of the deviatoric stress tensorτ. Note that in the yield state Equation (3) leads to$\tau_{rr} = -\tau_{zz}$.

Considering that the interface with the horizontal plane is a yielding surface, and that the deposit material in contact with the air is at atmospheric pressure$p = 0$, the following boundary conditions are obtained at the base of the deposit $z = 0$ and at the surface of the deposit$z = h(r)$.

$$\tau_{rz} = \tau_Y \qquad \text{on } z = 0, \tag{7}$$

$$\tau_{zz}\frac{\partial h}{\partial r} + \tau_{rz} + p\frac{\partial h}{\partial r} = 0 \qquad \text{on } z = h, \tag{8}$$

$$\tau_{rz}\frac{\partial h}{\partial r} - \tau_{zz} + p = 0 \qquad \text{on } z = h. \tag{9}$$

Loosely following [8], the order of magnitude of the different terms in Equations (3-9) can be studied selecting representative scales for the problem: $R$the final deposit radii, for the radial coordinate; $H_{R/2}$the height of the slump at some arbitrary radii (later it will be shown that this radii is$R/2$) for z and$h(r)$; $\tau_Y$for the shear stresses; and $\rho g H_{R/2}$ for$p$. Using this scales, two dimensionless parameters are defined$\in = H_{R/2}/R$, and$\gamma = \rho g H_{R/2}^2/(\tau_Y R)$; and Equations (4-9) can be rewritten in terms of dimensionless variables (note that the same notation is kept for the now dimensionless variables)

$$-\gamma\frac{\partial p}{\partial r} - \in\frac{\partial \tau_{zz}}{\partial r} + \frac{\partial \tau_{rz}}{\partial z} - \in\frac{\tau_{zz}}{r} = 0, \tag{10}$$

$$-\gamma - \gamma\frac{\partial p}{\partial z} + \in^2\frac{\partial \tau_{rz}}{\partial r} + \in\frac{\partial \tau_{zz}}{\partial z} + \in^2\frac{\tau_{rz}}{r} = 0, \tag{11}$$

$$\tau = 1, \tag{12}$$

$$\tau_{rz} = 1 \qquad \text{on } z = 0, \tag{13}$$

$$\in\tau_{zz}\frac{\partial h}{\partial r} + \tau_{rz} + \gamma p\frac{\partial h}{\partial r} = 0 \quad \text{on } z = h, \tag{14}$$

$$\in^2\tau_{rz}\frac{\partial h}{\partial r} - \in\tau_{zz} + \gamma p = 0 \qquad \text{on } z = h. \tag{15}$$

Under usual slumping conditions$\in \ll 1$, and$\gamma = 1$, if $H_{R/2}$ is appropriately selected. As $\in$ is small we look for approximate analytical solutions using power series and perturbation analysis. The power series expansions of the unknown solutions are

$$p = p_0 + \in p_1 + O(\in^2), \tag{16}$$

$$\tau_{zz} = \tau_{zz0} + \in\tau_{zz1} + O(\in^2), \tag{17}$$

$$\tau_{rz} = \tau_{rz0} + \in\tau_{rz1} + O(\in^2), \tag{18}$$

$$h = h_0 + \in h_1 + O(\in^2), \tag{19}$$

wherep_0, p_1, τ_{rr0}, τ_{rr1}, τ_{rz0}andτ_{rz1}, are functions of r and$z$, and h_0 and h_1 are functions of$r$.

Substituting these solutions into Equations (10-15) and keeping only the terms of order $O(\in^0)$ the following equations and boundary conditions are obtained

$$-\gamma\frac{\partial p_0}{\partial r} + \frac{\partial \tau_{rz0}}{\partial z} = 0, \tag{20}$$

$$\frac{\partial}{\partial z}(p_0 + z) = 0, \tag{21}$$

$$\tau_{zz0}^2 + \tau_{rz0}^2 = 1, \tag{22}$$

$$\tau_{rz0} = 1 \qquad \text{on } z = 0, \tag{23}$$

$$\tau_{rz0} + \gamma p_0\frac{\partial h_0}{\partial r} = 0 \qquad \text{on } z = h, \tag{24}$$

$$p_0 = 0 \quad \text{on } z = h. \tag{25}$$

The zero order solutions are then

$$p_0 = h - z, \tag{26}$$

$$\tau_{rz0} = 1 + \gamma\frac{\partial h_0}{\partial r}z, \tag{27}$$

$$\tau_{zz0}^2 = 1 - \left(1 + \gamma\frac{\partial h_0}{\partial r}z\right)^2, \tag{28}$$

$$h_0^2 = \frac{2}{\gamma}(1 - r). \tag{29}$$

Equation (29) gives the shape of the slump in the yielded region. Now, rewriting Equation (29) back in terms of dimensional variables, the zero order solution is

$$h^2(r) = 2\frac{H_{R/2}^2}{R}(R - r) = 2\frac{\tau_Y}{\rho g}(R - r). \tag{30}$$

Note that as$\gamma = 1$, we find that$H_{R/2} = h(R/2)$, which justifies the previously selected name.

Rearranging Equation (30) we obtain an expression for τ_Y as function of the shape of the slump

$$\tau_Y = \rho g\frac{h^2(r)}{2(R - r)}. \tag{31}$$

[8],used the slipline theory in order to construct the final shape of the deposit for a visco-plastic material. This approach required the consideration of rigid plug regions both near the center and the end of the deposit profile. The plug regions are evident in the experiments and show that the hypothesis of the material yielding at every point, as assumed in [10],asymptotic solutions, would only be valid

over some particular regions of the deposit. However, some region near the edge of the deposit can always be expected to have yielded and Equation (31) to apply over it.

Equation (31) may be compared with the expression presented by [10], which is a global equation based solely on final height of the deposit

$$\tau_Y = \sqrt{\frac{2\pi}{15V}}\rho g H^{5/2}, \tag{32}$$

where V is sample volume.

If the deposit volume is approximated as $V = \alpha\pi R^2 H$, with α as shape parameter (smaller than one), and it is replaced in Equation (32) we obtain

$$\tau_Y = \rho g\sqrt{\frac{2}{15\alpha}\frac{H^2}{R}}. \tag{33}$$

In general Equation (33) depends on the parameter α, which could change for samples with different composition or for slump test performed with container of different shape.

On the other hand, evaluating Equation (31) at $r = 0$ we obtain

$$\tau_Y = \frac{\rho g}{2}\frac{H^2}{R}, \tag{34}$$

which depends both on $H = h(0)$ and R. Furthermore, Equation (34) may be obtained from Equation (33) if $\alpha = 8/15$.

3. Methodology and experiments

The experimental procedure used for the experiments presented herein was as follows: first, a bottomless cylindrical container was placed over an horizontal rigid plane; then, the container was filled with a mud sample and let it to rest; finally, the container was quickly lifted allowing the material to slump.

The experiments were performed at the Instituto de Mecánica de los Fluidos e Ingeniería Ambiental (IMFIA) using both kaolinite and Montevideo's Bay natural mud. Water was added to the sediment samples in order to obtain different mud densities. PVC pipes (10 *cm* height and 9.5 *cm* internal diameter) were used as containers. High resolution measurements of the final deposit profile $h(r)$ were obtained by slicing the deposit with a sharp pre-wetted metallic blade and recording the slump profile with a 12.1 Megapixel digital camera (Lumix DMC-ZR1, Panasonic) as shown on Figure 2 left panel. A rectangular grid previously drawn on the blade allowed to remove the image distortion during image post processing.

The images were orthorectified using a homography transformation in order to have an image where the sliced plane has a constant scale. After image rectification, the profile was digitalized to obtain h as function of $R - r$. An example of a digitalized profile is shown in Figure 3. A least squares fit of Equation (31) to a portion of the digitized profile close to its edge was performed and the value of $\frac{\tau_Y}{\rho g}$ was computed. Finally, the sample density ρ was independently determined using a laboratory scale (LJ16 Infrared Dryers, Mettler Toledo).

Yield strength determinations using a vane geometry rheometer [DV-III ULTRA, BrookField) were performed simultaneously to the slump tests. The definition proposed by Migniot and Hamm [13],for computing τ_Y was used. In this definition τ_Y is associated with the maximum shear stress recorded during a constant low shear test. For this purpose, a homogenized sample was introduced in the rheometer, and after 3 minutes the vane rotation was started at 0.05*rpm*. The vane geometry used in the experiments was 2.535 *cm* height and 1.267 *cm* diameter.

Figure 3 shows the comparison between the proposed image analysis technique (Equation 31) and the rheometer results. Yield strength estimations using Equation (32) by [10], which uses only he final deposit height, are also included in Figure 3.

4. Discussion

Considering the [13],definition as an accurate proxy for τ_Y, Figure 3 shows that the image analysis technique gives a better and more consistent estimation of τ_Y than the simplified methodologies that relay just on one parameter (Equation 32). It is also relevant to note that estimations obtained with the image analysis technique show a unique relation with the rheometer estimations, while estimations obtained using [10],

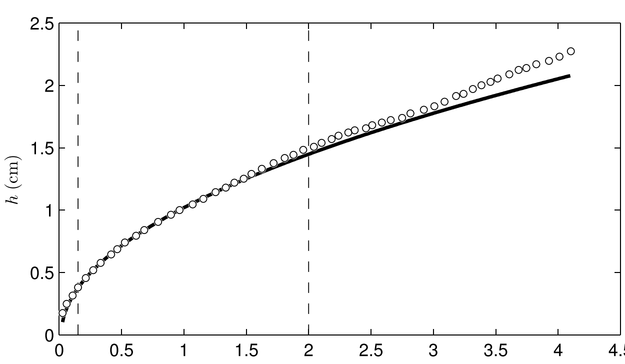

Figure 2. A digitized profile (o) and its least square fit (solid line) fitted over the yielded region (indicated with vertical dashed lines).

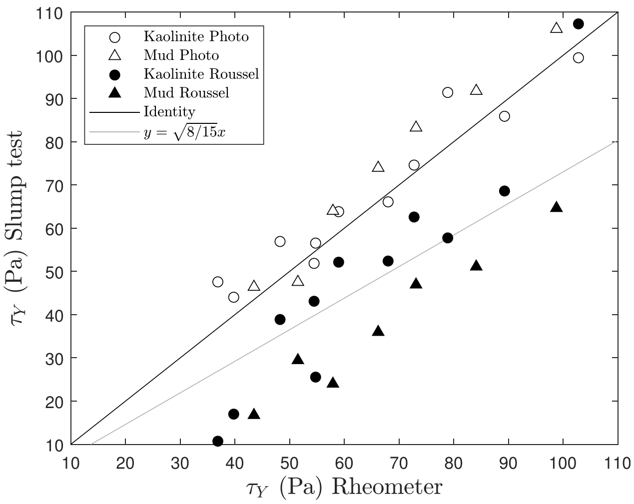

Figure 3. Yield strength estimations for kaolinite (○) and Montevideo's Bay mud (Δ) using the proposed image based technique [Photo) compared against vane rheometer estimations using 13,technique. Also shown, yield strength estimations for kaolinite (●] and Montevideo's Bay mud [△) using [10], formulation (Equation 32).

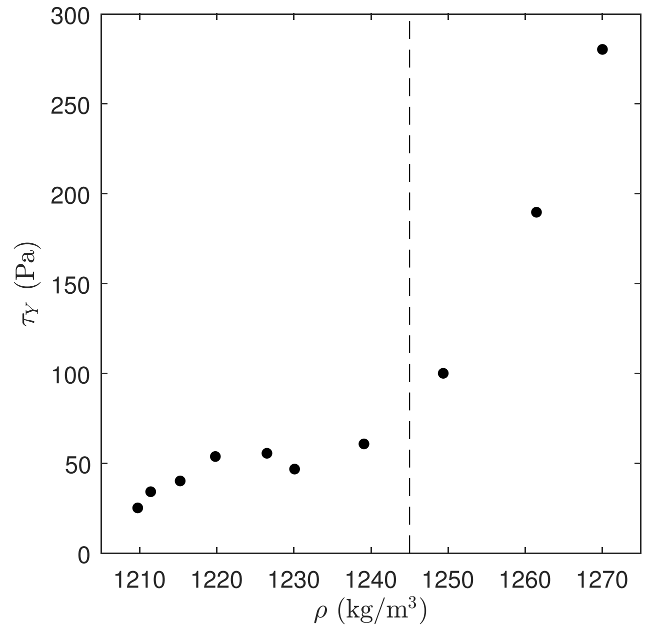

Figure 4. Determination of the mud density associated with the rheological transition for a mud sample from one of the navigation channels at the Port of Montevideo, Uruguay. The rheological transition [a mud density of 1245 kg/m^3) is indicated with a vertical dashed line.

formulation produces different relations depending on the sample composition.

It may be observed that yield strength values obtained with the image analysis technique tend to be slightly larger that the ones obtained from vane rheometer measurements. This discrepancy may have to do with the [13],definition of τ_Y itself, and it may by solved by just subtracting a small constant value [5 Pa) to the yield strength determined from the slump test.

A strong limitation of [10],methodology is that it assumes that the whole the sample has yielded, which is hardly verified, particularly for samples with high τ_Y values. The image analysis technique, on the other hand, assures that the region that is being analyzed has yielded, which results in its better performance.

It is possible that the use of a blade to cut the deposit and facilitate the measurement of the profile may slightly perturb the shape of the deposit. This could be avoided with the use of a low power laser for generating plane light sheet and a frame to fix it to the camera as described in [14],for bathymetry measurements.

The proposed methodology was used during a field study for the determination of the nautical depth in the Montevideo Port [15]. During this study, muds with different densities from the Montevideo Port navigation channel were used to study the relation between τ_Y andρ. Analyzing the results, an inflection point, where yield strength decreased abruptly with a small decrease of density, was found (Figure 4). This showed the existence of a rheological transition, and a mud density that can be associated with it. The rheological transition is used for the definition of the nautical depth based on the mud density, and the nautical bottom is defined as the depth where the mud density reaches that particular density value [16].

5. Conclusions

The determination of the yield strength of a mud sample from the final height of a slump deposit was reviewed, and a new image analysis based technique was proposed. The use of the deposit profile instead of a global dimension of the deposit to characterize the material assures that the area of the deposit that is being analyzed has yielded, giving a much more accurate estimation of the mud yield strength than [10],technique, which only uses the deposit height.

The proposed methodology it is particularly useful for the study of non-homogeneous material, mixes of sand and gravel with mud for example, where the analysis of a large sample is needed in order to obtain a global characterization of the material. While the image analysis technique may be harder to use in the field than the [10],technique, it may be easily implemented for routinely use in the laboratory. It may also be automatized using a frame, a laser with cylindrical lens, and a camera; and developing some user friendly software that facilitates the rectification of the image and the fitting of the analytical profile.

Acknowledgments

The authors would like to thank the Agencia Nacional de Investigación e Innovación (ANII], Uruguay, for the financial support given to the first author under its scholarships program Becas de Posgrados Nacionales and the research program Fondo María Viñas. Also thanks to the Laboratorio de Materiales, of the Instituto de Ingeniería Química of the Facultad de Ingeniería. Thanks to the CAPES-UdelaR academic exchange program (026/2010) of the CAPES Foundation, Brazil, and the Universidad de la República, Uruguay, which allows the work with the Laboratório de Dinâmica de Sedimentos Coesivos (LDSC), Universidade Federal do Rio de Janeiro.

The field work was performed during an outreach project between the Universidad de la República and the Adminsitración Nacional de Puertos (ANP). The support of Katoen Natie, Uruguay during that project is also gratefully acknowledged.

We would also like to thank Aldo Bologna, Marcos Gallo, Valentina Groposo, Thiago Leão, Ismael Piedra-Cueva, Gustavo Sánchez, Manuel Teixeira and Susana Vinzón for making the work presented here possible.

Disclosure statement

No potential conflict of interest was reported by the author(s).

ORCID

Rodrigo Mosquera http://orcid.org/0000-0001-8036-8400

References

[1] ASTM. 2003a. Astm c143/c143m-05 - standard test method for slump of hydraulic cement concrete. [Computer software manual]. West Conshohocken, PA.
[2] ASTM. 2003b. Wk27311 - new test method for measurement of cement paste consistency using a mini-slump cone. [Computer software manual]. West Conshohocken, PA.
[3] Liu Y, Balmforth N, Hormozi S. Axisymmetric viscoplastic dambreaks and the slump test. J Non-Newtonian Fluid Mech. 2018;258:45–57.
[4] Pashias N, Boger D, Summers J, et al. A fifty cent rheometer for yield stress measurement. J Rheol. 1996;40:1179–1189.
[5] Murata J. Flow and deformation of fresh concrete. Mater Struct. 1984;17:117–129.
[6] Balmforth NJ, Craster RV, Rust AC, et al. Viscoplastic flow over an inclined surface. J Non-Newtonian Fluid Mech. 2006;139:103–127.
[7] Clayton S, Grice T, Boger D. Analysis of the slump test for on-site yield stress measurement of mineral suspensions. Int J Miner Process. 2003;70(1–4):3–21.
[8] Dubash N, Balmforth NJ, Slim AC, et al. What is the final shape of a viscoplastic slump. J Non-Newtonian Fluid Mech. 2009;158:91–100.
[9] Pierre A, Lanos C, Estelle P. Extension of spread-slump formulae for yield stress evaluation. Appl Rheol. 2013;23:6.
[10] Roussel N, Coussot P. Fifty cent rheometer for yield stress measurements: from slump to spreading flow. J Rheol. 2005;49:705.
[11] Schowalter WR, Christensen G. Toward a rationalization of the slump test for fresh concrete: comparisons of calculations and experiments. J Rheol. 1998;42:865.
[12] Eirich FR. Rheology: theory and applications. New York: Academic Press; 1956.
[13] Migniot C, Hamm L. Consolidation and rheological properties of mud deposits. Coastal Eng Proc. 1990;1:2975–2983.
[14] Spinewine B, Delobbe A, Elslander L, et al. Experimental investigation of the breach growth process in sand dikes. In: Proceedings of the Second International Conference on Fluvial Hydraulics. Vol. 2, River Flow: CRC Press; 2004. p. 983–991.
[15] Groposo V, Mosquera R, Pedocchi F, et al. Mud density prospection using a tuning fork. J Waterw, Port, Coastal, and Ocean Eng. 2015;141(5):4014047.
[16] PIANC. Harbour approach channels—design guidelines. Brussels, Belgium: World Association for Waterborne Transport Infrastructure; 2014. (Tech. Rep. No. Report No. 121).